INTERFEROMETRIC AND POLARIMETRIC OBSERVATIONS OF WINTER FORESTS

Dimitra Panagiotopoulou[1], and Ian A. Brown[2]

1. University of Stockholm, Department of Physical Geography, Stockholm, Sweden; dimitra.panagiotopoulou@hotmail.com
2. University of Stockholm, Department of Physical Geography, Stockholm, Sweden; Ian.Brown@natgeo.su.se

ABSTRACT

The accuracy of TanDEM-X (TDX) interferometric SAR data acquired during winter was tested over a sub-Arctic site in Norway. 14 image pairs were analysed, 12 of which were bistatic HH-pol data. Two monostatic quad-pol scenes, one of which was acquired over the Hemavan/Tärnaån region of Sweden, were also processed. Digital elevation models (DEMs) generated from the data typically display height errors of < 1m relative to a reference DEM. No relationship was found between DEM surface height and snow cover. Principal components analysis found that interferometric coherence was strongly related to snow depth and backscatter intensity was related to forest parameters such as diameter at breast height and stand density. Phase differences between HH and VV-pol data were correlated with snow depth over the Norwegian site though not over the Swedish site. The result show that TDX DEMs routinely achieve very high vertical accuracy. TDX coherence is strongly affected by snowpack parameters suggesting TDX coherence inversion may enable snow cover monitoring.

INTRODUCTION

Snowpack monitoring at high latitudes is important to water resource management, hazard mitigation (floods and avalanches), infrastructure maintenance, climate science and weather forecasting. Optical systems may face limits to their effectiveness due to persistent cloud cover and short periods of solar illumination in winter. Active microwave systems, and especially Synthetic Aperture Radar (SAR) systems are sensitive to snowpack parameters and are unaffected by cloud and the polar night.

SAR Interferometry (InSAR) utilises the phase difference between two SAR acquisitions obtained over the same location [1] to produce an interferogram [2, 3]. InSAR is a technique in which the scattering centre elevation is measured by exploiting the small phase differences between two SAR acquisitions made from spatially separated locations at either end of a baseline, and thus at slightly different incidence angles [1]. Thus, it becomes possible to investigate surface topography as well as the assessment of physical surface changes to within a fraction of wavelength, by exploiting the phase of the coherent radar signal [3]. Singh et al. [4] analysed SIR-C/X-SAR data, observed that snowfall, snow metamorphosis, and densification sharply lead to a degradation of interferometric coherence of within a few days. In the case of high interferometric coherence, differences in phase caused by the signal delay of snow can be analyzed [5, 6]. Significant height errors in InSAR derived DEMs from ERS-1/2 tandem data over glaciers, ice sheets and bare ground may be attributable to snowfall events and/ or to small changes in snow properties between acquisitions. Guneriussen et al. [6] originally defined the theoretical relationship between interferometric phase and changes in SWE resulting in DEM height for ERS-1/2 tandem configuration.

Single-pass InSAR systems have the advantage of low temporal decorrelation but, they require multiple SAR sensors in a close flying formation. An example is the TanDEM-X system comprising

TerraSAR-X and TanDEM-X platforms, operated by the German Aerospace Center (DLR) [7]. The primary objective of the TanDEM-X (TerraSAR-X add on for Digital Elevation Measurements) mission is to provide the first global, high resolution Digital Elevation Model (DEM) with an unprecedented accuracy, which is equaling or surpassing the HRTI-3 specification. The orbit configuration based on a Helical geometry [8]. Such configurations eliminate geometric and radiometric distortions, easier pointing and timing synchronization [9].

This study investigates on the sensitivity of TanDEM-X based interferometry on snow covered terrain. The key aspects of consideration for the analysis were the spatiotemporal consistency of interferometric phase differences by means of elevation values and interferometric coherence (γ), and the identification of principal contributors of the phase variation related to given snowpack variables. The TDM observations, were evaluated by means of absolute and relative vertical accuracy. Although it was anticipated that the height error estimations would be below the required accuracy for TanDEM-X mission, investigations on the X- band backscattering signatures and height sensitivity over snow-covered surfaces can offer new potentialities for the SAR snow investigations. In addition, the correlation between polarimetric phase differences and snow depth was investigated on quad-polarised TanDEM-X SAR data.

METHODS

Test sites

The study carried out at Daja Valley (67° 5' N, 16° 2' E) in Fauske municipality, Norway. The site is a glaciogenic U-shaped valley with forest cover in the valley interspersed with mires and open heath above the treeline. Forest species consist primarily of birch (*Betula spp*.) and Norway spruce (*Picea abies (L.) Karst*). The sampled locations were located in the valley (slope < 20%), in order to the exclude any topographic effects that induce geometric and radiometric distortions. The test sites can be grouped into three general land cover classes, open terrain (mire), coniferous and deciduous stands. The second site, Tärnaån valley is near Hemavan, northern Sweden (65° 8' N, 15° 4' E). The valley is a sub-Arctic landscape with birch forest at the southern (lower) extremity and heath extending northwards. A lake and wetland is located at the northern end of the site. The valley is bounded to the west by mountains.

TanDEM-X SAR Datasets

TDX data were received from DLR in CoSSC (co-registered single-look slant range complex) format with common spectral filtering applied during pre-processing. Thirteen bistatic stripmap (SM) single polarized (Sp) (HH/HH) acquisitions were received. The effective baseline varied from 39 to 83 m within the dataset, which were all well below the half of the critical baseline. The height of ambiguity (HoA) varied from 63 to 142 m. The Doppler Centroid differences for each transmitter – receiver pair were less than the half of the Pulse Repetition Frequency (PRF). The pixel spacing in the CoSSC data varied from 0.91 to 1.36 m in range and from 1.73 to 1.98 in azimuth. The initial bistatic TDX resolution varied from 2.11 to 2.71 in ground range with a constant Doppler resolution of 3.29 m.

The second dataset consisted of two SM quad-polarized acquisitions in pursuit monostatic interferometric mode. The pixel spacing was 2.48 m in range and 1.36 in azimuth. The initial obtained TDM resolution varied from 3.89 to 4.24 in ground range with a constant Doppler resolution of 6.59 m.

Data Processing

A differential interferogram was calculated for each TDX pair by subtracting the constant interferometric phase due to dynamic range and topography from the interferogram. For this, interferometric phase was simulated exploiting an external DEM with a grid spacing of 10 m for Daja Valley and 25 m for Hemavan test site. The DEM was interpolated in radar geometry using the precise satellites orbits and the ZDTs calculated during the pre-processing [10]. The differential

interferograms were pre-filtered with the modified Goldstein adaptive filter [10] which optimise the detectability of fringe cycles and eliminates phase noise. Phase unwrapping of the differential interferograms was performed using a branch cut based phase unwrapping algorithm, namely Minimum Cost Flow (MCF) [11]. The unwrapped differential interferograms re-combined with synthetic phase, were corrected with a phase offset, then converted to elevation and geocoded.

In addition to interferometric processing, backscattering coefficient (σ^0) were computed for both datasets. Intensity images were filtered using a 5 x 5 pixel Refined Lee Filter. The intensity data were then radiometrically corrected and geocoded using the external DEM. Each pixel was normalised for the real illuminated area of each resolution cell. The correction for the antenna gain pattern in range was based on topography; the data were also corrected for range spread loss. During both interferometric and intensity processing, multi-looking approach applied with the number of looks varying from 3 to 6 in range and from 4 to 5 in azimuth, corresponding to an approximating pixel size of 10 m, as the resolution for the final geocoded interferometric product.

For the quad-pol dataset, Polarimetric Phase Difference ($\Delta\gamma$) was computed using co-polarized master and slave data (HH/VV polarizations). Inter-channel coherence (γ), was calculated. γ is the magnitude of correlation coefficient and is a measure of similarity between two images. The phase of the correlation coefficient contains information about the vertical distribution of the scatterers. The total coherence magnitude for a given measurement is affected by the decorrelation due to noise, vertical spread of the scatterers and temporal decorrelation. Concerning that volume decorrelation is a geometric effect caused by the distribution of scatterers in vertical direction.The resulting products, InSAR derived DEMs, coherence images, master SAR images and $\Delta\gamma$, were all geocoded, considering the Range-Doppler equations.

Height Error Analysis

The estimation of the absolute vertical accuracy was undertaken based on the computation of the absolute height error, which was defined as the difference between the InSAR elevation of the respective experimental DEM product and the value of the reference DEM (the external DEM). Additionally the relative vertical accuracy, as second indicator of uncertainty was taken into account by the computation of the relative or point-to-point height errors, where the point-to-point was referred to one resolution cell whose elevation value is the average of elevation values of all underlying pixels; the 90th percentile of relative vertical height error was estimated between two InSAR DEMs with same acquisition configuration.

Principal Component Analysis

Prinicpal Components Analysis (PCA) was applied to the variables describing the radar response and target. PCA is a procedure for identifying hypothetical variables (components), which account for the variance in a multidimensional dataset; these new variables are linear combinations of the original variables. PCA was performed for each land cover category for all the acquisitions by encompassing variables such as the variation in σ^0, γ, Local Incidence Angle (LIA), as well as the temporal observations of snow parameters, namely snow depth (SD), Snow Water Equivalent (SWE). Diameter at Breast Height (DBH) used as supplementary variable for the forest stands.

Variables that were strongly correlated ($r \geq 0.5$) with the first component considered more significant, and thereby can be assumed as the driving forces of changes in interferometric pattern. Additionally, the interpretation of relationship among the variables based on the criterion Jolliffe cut-off value, i.e., it gives an informal indication of how many principal components should be considered significant [12]. Thus, components with eigenvalues smaller than this value were considered insignificant.

RESULTS

The interferometric surface heights derived from TDX pairs all conformed to the TDX user requirement of < 2m. An analysis of pairs with similar acquisition parameters (e.g. HoA and band width) showed 90th percentile differences of ≤ 0.5 m for all but one comparison (InSAR DEMs from

20120122 and 20120202). The 20120122 dataset was the worst performing of all the TDX interferometric pairs (Table 1).

Table 1: Mean absolute height error (HE) and 90 percentile absolute HE over three landcover classes in Daja. The lowest HEs are found over open terrain where the absence of scattering from vegetation canopies results in greater accuracy.

Acquitision date	*Absolute HE (90%) (m)*			*Mean absolute HE (m)*		
	Open (768 pixels)	*Deciduous (808 pixels)*	*Coniferous (510 pixels)*	*Open (768 pixels)*	*Deciduous (808 pixels)*	*Coniferous (510 pixels)*
20120117	0.83	1.51	1.51	0.43±0.38	0.66±0.57	0.73±0.60
20120122	1.30	1.29	1.51	0.61±0.55	0.63±0.49	0.71±0.59
20120123	0.67	1.67	1.52	0.36±0.43	0.72±0.59	0.74±0.56
20120128	0.82	1.54	1.48	0.44±0.35	0.67±0.57	0.72±0.64
20120202	0.90	1.64	1.64	0.49±0.40	0.73±0.63	0.74±0.64
20120203	0.64	1.57	1.50	0.37±0.46	0.67±0.57	0.73±0.57
20120208	0.68	1.60	1.44	0.35±0.36	0.71±0.58	0.71±0.53
20120301	0.87	1.56	1.50	0.45±0.40	0.68±0.58	0.75±0.63
20120306	0.96	1.57	1.48	0.49±0.40	0.69±0.63	0.73±0.62
20120317	0.97	1.61	1.54	0.49±0.40	0.72±0.64	0.75±0.64
20120328	0.94	1.56	1.58	0.47±0.37	0.7±0.63	0.76±0.66
20120619	0.65	1.53	1.44	0.36±0.39	0.7±0.58	0.71±0.54
20130315	0.97	1.59	1.59	0.50±0.39	0.69±0.63	0.76±0.65

PCA was applied to the data to analyse the relationships between variables. For sites classed as Open landcover PCA1 explained 45% of the variance and PCA2 32%. For Deciduous stands the variance explained was PCA1 35%, PCA2 23% and RCA3 18%. For Coniferous stands the values were: PCA1 36%, PCA2 21% and PCA3 20%. Loadings describing the correlations between variables and components show that for each of the landcover classes γ was more important to PCA1 than σ^0 (-0.7, -0.7 and -0.8 for Open, Deciduous and Coniferous respectively). Of the target variables snow depth (0.8, 0.9 and 0.9) and local incidence angle (-0.5, -0.6, -0.5) were important. For the forest classes DBH and number of stems were important loadings for PCA2 with negative correlations for DBH and positive for number of stems. Backscatter was a more significant loading for PCA2 than coherence. The importance of allometric descriptors and their inverse relationships suggests that σ^0 is more sensitive to dense copse-like stands that larger trees widely spaced. The

importance of snow cover to coherence is shown in PCA1 across all landcover types. This emphasises the potential of interferometric products for snowpack investigations.

The dielectric properties of snow at 9.65 GHz vary significantly with respect to liquid water volume fraction [13]. Snowpacks are typically comprised of different snow layers which are not necessarily homogenous and horizontally structured. Dry snow is highly transparent for X- (8-12.5 GHz), and the main backscatter signal derives from the underlying ground surface [14]. However, there is a signal delay due to the refraction occurred within the snow volume and thus results in an interferometric phase difference which can be associated to changes in snow parameters [6]. However, the polarimetric signature of a surface is not affected when the surface is covered by a homogeneous and transparent medium, differential polarimetric phase delays related to the refraction index of snowpack might be introduced.

For Daja there is typically a negative phase difference ($\Delta\gamma$) between HH and VV pol data suggesting layering in the snowpack has resulted in a longer path for the HH-pol data, which might be expected. At the Tärnaån site the phase difference between HH and VV data is less uniform and the magnitude of difference is greater than in Daja. The Daja $\Delta\gamma$ was found to be correlated with snow depth in the forest sites using a robust least-squares fit ($r^2 = 0.89$). At Tärnaån there was no significant relationship to snow depth. However, it should be noted that the snowpack data were from a previous year (though repeated observations have shown the spatial distribution of snow to be persistent).

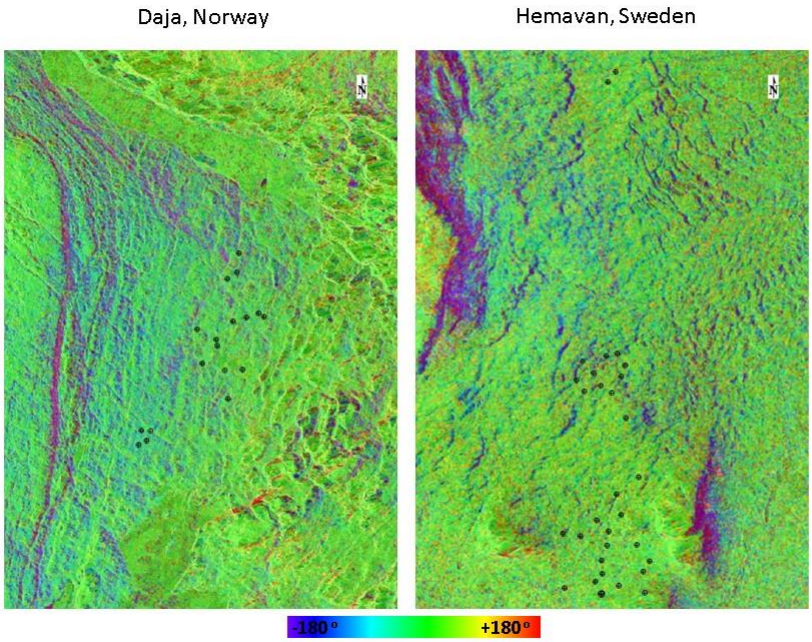

Figure 1: Phase difference between HH and VV-pol data over the two study sites, Sampling locations are marked..

CONCLUSIONS

The results presented here show that TDX InSAR repeatedly out-performs the stated user requirement of DEM accuracy < 2 m. Height errors of < 1 m were routinely achieved. PCA showed the TDX γ and snowpack parameters to be correlated. $\sigma°$ was most affected by forest variables; stand density was positively correlated with $\sigma°$ and DBH negatively. The sensitivity of TDX X-band data to snowpack variables is established. Preliminary results suggest $\Delta\gamma$ and snow depth may be

correlated. TDX offers exciting opportunities to further investigate advanced SAR methods for snow cover analyses.

ACKNOWLEDGEMENTS

This research was funded by the Swedish National Spaceboard and Carl-Fredrik von Horns fond whose support is gratefully acknowledged.

REFERENCES

[1] R. Bamler and P. Hartl, “Synthetic aperture radar interferometry,” *Inverse Problems*, vol. 14, pp. R1–R54, 1998.
[2] R. F. Hanssen, *Radar Interferometry: Data Interpretation and Error Analysis*. The Netherlands: Kluwer, 2001.
[3] P. A. Rosen, S. Hensley, I. R. Joughin, F. K. Li, S. N. Madsen, E. Rodriguez, and R. M. Goldstein, “Synthetic aperture radar interferometry,” *Proc. IEEE,* vol. 88, pp. 333-382, 2000.
[4] G. Singh, G. Venkataraman, Y. S. Rao, and V. Kumar, and Snehmani, “InSAR coherence measurement techniques for snow cover mapping in Himalayan region,” *in IEEE International, Geoscience and Remote Sensing Symposium (IGARSS)*, Boston, MA, 7-11 July 2008, vol. 4, pp. IV – 1077, IV – 1080.
[5] S. Li and M. Sturm, “Derivation of spatial distribution of snow precipitation using interferometric SAR technique,” *in Proc. IEEE International Geoscience Remote Sensing Symposium (IGARSS)*, Sydney, NSW, 09 -13 July 2001, vol. 4, pp. 1795–1797.
[6] E. J. Deeb, R. R. Forster, and D. L. Kane, “Monitoring snowpack evolution using interferometric synthetic aperture radar on the North Slope of Alaska,” *Int. J. Remote Sens.,* vol. 32, no. 14, pp. 3985–4003, 2011.
[7] T. Guneriussen, K. A. Høgda, H. Johnsen, and I. Lauknes, “InSAR for estimation of changes in snow water equivalent of dry snow,” *IEEE Trans. Geosci. Remote Sens*., vol. 39, no. 10, pp. 2101–2108, October 2001.
[8] R. Werninghaus and S. Buckreuss, “The TerraSAR-X mission and system design,” *IEEE Trans. Geosci. Remote. Sens.*, vol. 48, no. 2, pp. 606–614, 2010.
[9] A. Moreira et al., “TanDEM-X: TerraSAR-X Add-On for Digital Terrain Elevation Measurements”. Mission Proposal for a Next Earth Observation Mission. DLR Document No. 2003-3472739, November 2003.
[10] M. Zink and A. Moreira, “TanDEM-X mission status: The new topography of the earth takes shape,” in *IEEE International Geoscience and Remote Sensing Symposium (IGARSS),* Quebec City, QC, 13-18 July 2014, pp. 3386 – 3389.
[11] S. Duque, U. Blass, C. Rossi, T. Fritz and W. Balzer, “TanDEM-X payload ground segment, CoSSC generation and interferometric considerations,” Remote Sensing Institute, German Aerospace Center (DLR), Tech. Rep., 2012.
[12] C. Prati and F. Rocca, “Improving slant range resolution of stationary objects with multiple SAR surveys,” *IEEE Trans. Aerospace Electron. Syst*., vol. 29, pp. 135-144, January 1993.
[13] I. T. Jolliffe, *Principal Component Analysis*. Springer-Verlag, 1986.
[14] T. Abe, Y. Yamaguchi, and M. Sengoku, “Experimental study of microwave transmission in snowpack,” *IEEE Trans. Geosci. Remote Sens.*, vol. 28, no. 5, pp. 915–921, September 1990
[15] J. Shi, J. Dozier, and S. Hensley,” Mapping snow cover with repeat pass synthetic aperture radar,” in *IEEE International Geoscience and Remote Sensing Symposium (IGARSS),*1997*,* Singapore, vol. 2, pp. 628−630.